? this L wrt R. low values of L.
exptl. results on fracture?

PAPER 7 (SESSION I)

Notch brittleness and plastic constraint factor in mild steel

H. TAKAHASHI
Tohoku University, Sendai, Japan

Summary

The tensile fracture behaviour in mild steel at low temperature has been studied with a photo-elastic technique. The plastic constraint factor proposed by Orowan was determined from the inhomogeneous plastic deformation, and the notch brittleness at low temperature can be associated with this factor. In a notched specimen under tensile deformation there is always a plastically constrained zone and an unconstrained zone for the propagation of plastic yielding near the notch roots. In particular, the consecutive change of plastic constrained state was revealed from the stress dependence of the development of plastic deformation from the unconstrained zone into the constrained zone. The value of the plastic constraint factor of the notched specimen is about 1·1 at room temperature, although it increases with decreasing temperature. Thus the plastic constraint factor may be a practical measure of the fracture strength at low temperature and therefore applicable to engineering design.

Introduction

The classical theory of notch brittleness defines the conditions under which brittle fracture can occur in a potentially ductile material. Based on these theoretical considerations, Orowan [1] has given a qualitative explanation for cleavage fracture in a notched specimen using a plastic constraint factor, which is a measure for estimating hydrostatic component under triaxial stress system. The plastic constraint factor is defined as the value of the nominal stress across the minimum section divided by the uniaxial yield stress of a smooth specimen, when plastic zones have traversed the notched specimen and the specimen is in a state of general yield.

In various theoretical treatments plastic constraint factors for several shapes of notch have been calculated by the solutions of elastic-plastic problems under plane stress or plane strain condition. However, the application of the theoretical plastic constraint factor to engineering problems, such as machine or structural design, may be limited because of the complexity of the stress system and of the mechanical properties of materials. It has been shown that the plastic constraint factor depends not only on the notch geometry or triaxial stress, but also on the yield strength or plastic behaviour of the metal. These properties are dependent on the deformation temperature and the plastic constraint factor must therefore be measured as a function of temperature. It is consequently of practical importance to

determine a plastic constraint factor of an actual material in a wide temperature range below room temperature.

Recently, the photoelastic coating technique has been used to investigate the elastic-plastic strain distribution on the surface of a flat specimen containing notches at room temperature [2, 3]. Dixon [3] has shown that the plastic constraint factor for any shape of notch can be deduced from the stress dependence of strain distribution obtained by photoelastic fringe patterns.

Recent approaches [4-7] to the problems of notch brittleness in mild steel have been directed towards the analysis of the plastic constraint due to hydrostatic stress in a notched specimen. There have been few quantitative investigations of the plastic constraint, since the true stress-strain relation has not yet been obtained for a complicated stress system.

In this study, successive changes of the plastic constrained state under tensile deformation of a notched specimen were measured using a low temperature photoelastic coating technique [8], and the plastic constraint factor was determined from the results. The temperature dependence of the fracture strength of a notched specimen was studied using the plastic constraint factor, from which the rise of the ductile-brittle transition temperature due to notch effect was estimated. It is suggested that the plastic constraint factor may be a practical measure of the fracture strength at low temperature and of importance in engineering design.

Photoelastic observations of low temperature deformation in mild steel

Two steels were used, of the following compositions, wt.-%:

	C	*Si*	*Mn*	*P*	*S*
Steel A	0·09	0·33	0·35	0·026	0·02
Steel B	0·004	0·32	0·34	0·026	0·02

Tensile notched specimens of thickness 2 mm and width 8 mm in minimum section, with notch depth 2 mm, notch root radius 0·07 mm and an included angle of 45° were machined from steel bars. Steel A was used in the 'as-received' state after machining, while steel B, after machining, was heat-treated for 60 hr at 950°C in a wet hydrogen atmosphere for decarburization, followed by furnace cooling. The notched specimens were deformed in uniaxial tension at various low temperatures, using a liquid-air cryostat [8] with a metal cage suspended from the cross-head of a Tensilon universal testing machine of 5 ton capacity. The metal cage was surrounded with a transparent cryogenic glass envelope, which enabled a temperature down to −180°C to be maintained within about ±1°C. The applied cross-head speed was 0·03 mm/min for all tension tests. Narmco Resin 7343/7139 was used as the photoelastic wafer material and the wafer of approximately

2 mm in thickness was bonded to the surface of the specimen with the same resin. The photoelastic fringe patterns obtained in the tension tests of steel A at room temperature and at −150°C are shown in Figs. 1 and 2 respectively. The variation of nominal stress across the net section is indicated as the stress ratio σ_N/σ_y, where σ_y is a nominal stress across the minimum net section and σ_y is adopted as the nominal yield stress in the state when the maximum principal strain difference at the notch root reaches to 1%, corresponding to the yield stress of the smooth specimen. From tension tests of several unnotched specimens at low temperature, it was confirmed that the localized yield stress of a notched specimen coincided with the macroscopic yield stress of a smooth specimen. In Fig. 2 (a) obtained at $\sigma_N/\sigma_y = 0$, an initial fringe pattern appears due to the thermal differential expansion of the substrate metal and the plastic wafer. Thus the principal strain differences at each loading stage can be obtained by subtracting the initial fringe from each fringe pattern. By comparing the deformation at room temperature with that at −150°C, it is obvious that the temperature and stress dependence of developments of plastic in mild steel exists. Even at −150°C, after a plastic deformation greater than 1% was observed, brittle fracture occurred in the minimum section. In the whole temperature range the initial development of plastic yielding from the notch roots always extended in a direction of 45° to the tensile axis.

Plastic constraint factor and its temperature dependence

In the plane strain deformation of a notched specimen there always appears a plastic 'hinge', whose schematic diagram is shown in Fig. 3. To discuss the consecutive change of plastic constraint with increasing load, three points 'A', 'E' and 'F' were chosen. 'A' is the most highly strained point under deformation. 'F' is an intersecting point of the center line of the specimen and the plastic 'wing' which traverses across the specimen with increasing load, and 'E' is the center of the minimum section.

Figs. 4 and 5 illustrate the variation of principal strain difference γ_A, γ_E and γ_F at the three points 'A', 'E' and 'F' respectively as a function of σ_N/σ_y at room temperature and −150°C. In these figures, it can be seen that the plastic flow takes place firstly at 'A', thereafter it propagates into 'F' with a forked shape. The plastic propagation into 'E' is restrained until the stress level in the minimum section is sufficient to overcome the hydrostatic component. In order to determine the plastic constraint factor, it has been necessary to point out the state of general yield when the plastic zones have completely developed across the specimen. The variations of the strain ratio γ_F/γ_E at the points 'E' and 'F' in reference with σ_N/σ_y are shown in the upper diagrams of Figs. 4 and 5. Using the results obtained at various temperatures in steel A and B, the temperature dependence of plastic propagation is illustrated in Figs. 6 and 7 respectively. At lower

stress levels than $\sigma_N/\sigma_y = 1{\cdot}1$, as shown in these figures, the plastic propagation from 'F' into 'E' is restrained because of plastic constraint of the notch even though the load is increasing, while the development from 'A' into 'F' is unconstrained. Therefore, the strain ratio γ_F/γ_E should increase with increasing stress in the whole temperature range. It is noticed, however, that the gradient of strain ratio curve increases rapidly with decreasing temperature in both mild steel and low carbon steel. At higher stress level than $\sigma_N/\sigma_y = 1{\cdot}1$, on the other hand, the strain ratio decreases with increasing load, where the plastic yielding propagates progressively and the constraint due to notch is relaxed with increasing plastic deformation of central portion. From this stress dependence of strain ratio curve $\gamma_F/\gamma_E - \sigma_N/\sigma_y$, it may be suggested, from the following evidence, that the general yield occurs at the extreme peak on the curve. With reference to the macroscopic load-elongation curve, it was found that the unrestricted plastic flow initiates at the load where a peak appears. It seems, reasonable, therefore that the value of the stress ratio σ_N/σ_y is to be defined as the plastic constraint factor.

The temperature dependence of the plastic constraint factor is shown in Fig. 8. The value of the plastic constraint factor is about 1·1 at room temperature, while it increases with decreasing temperature to 1·2 at about −150°C. Using Dixon's experimental data [3], the relationship between $\gamma_F/\gamma_E - \sigma_N/\sigma_y$ was calculated to compare the plastic constraint factor at room temperature obtained from this study with that given by Dixon. The result is represented by the dotted line in Fig. 6. It is also clear that γ_F/γ_E is a maximum at the value of $\sigma_N/\sigma_y = 1{\cdot}1$. The value of the plastic constraint factor agrees with that given by Dixon, although his investigation was limited only to a non-work-hardening material. It was observed, furthermore, that the brittle fracture occurred without the general yielding at the low temperature −150°C, as shown by the dashed curve in Fig. 6.

Estimation of transition temperature with plastic constraint factor

Orowan has given a successful explanation of the notch brittleness using the theoretical plastic constraint factor of 3. The rise of transition temperature due to notch effect can be estimated from his basic idea.

In Fig. 9 σ_F, σ_y and σ_{PCF} are plotted as functions of the temperature; σ_F represents the brittle fracture strength, σ_y the yield stress of smooth specimen in uniaxial tension. σ_{PCF} is the notch-constrained yield stress, which is obtained from σ_y and the plastic constraint factor determined by this experiment. In a smooth specimen the temperature at which the σ_y-curve intersects the σ_F-curve is labelled T_1, (that is approximately −180°C), while in the notched specimen the temperature at which the σ_{PCF}-curve crossed with the σ_F-curve increases to T_2. It is seen, therefore, that the ductile-brittle transition temperature rises from −180° to about −130°C.

The temperature rise is about 50°C in this experimental condition. The above result was also confirmed from the observation of fracture surface.

Plastic constraint factor and tensile strength in notched specimen

The nominal ultimate tensile strength of a notched specimen was determined from the load-elongation curve. In the temperature range, above −100°C, where plastic deformation and work hardening markedly appear, the nominal tensile load is increased with further increase of plastic strain. General yield in mild steel (steel A) at room temperature occurred at the load of $\sigma_N/\sigma_y = 1{\cdot}1$. From the load-elongation curve, on the other hand, it was shown that the value of σ_N/σ_y at the load corresponding to the ultimate tensile strength was about 1·4. At low temperature −150°C where the brittle behaviour of the specimen becomes prominent, the fracture load almost coincides with the plastic constraint factor $\sigma_N/\sigma_y = 1{\cdot}2$. According to the above consideration, the nominal tensile strength can be represented as the stress ratio $(\sigma_N/\sigma_y)_{UTS}$ at the maximum load. Other values of $(\sigma_N/\sigma_y)_{UTS}$ at various temperatures were obtained with the same procedure. The temperature dependence of $(\sigma_N/\sigma_y)_{UTS}$ in steel A is shown in Fig. 10.

In a low carbon steel yielding is initiated and then develops easily at small tensile load. This material is so ductile that a further large plastic deformation then appears. At −35°C, for example, even after yielding had occurred in the early stage of deformation, successive plastic deformation and work hardening took place until $(\sigma_N/\sigma_y)_{UTS}$ reached 3. At low temperature, however, below −160°C the fracture strength in low carbon steel also coincides with the plastic constraint factor, as occurs in mild steel. The temperature dependence of $(\sigma_N/\sigma_y)_{UTS}$ in steel B is also shown in Fig. 10. As can be seen in this figure, it is particularly interesting that the brittle fracture strength in mild steel and low carbon steel at low temperature can be deduced with the plastic constraint factor.

Discussion

It is important to consider the reinforcement effect of the photoelastic coating wafer on the deformation of material. It has been suggested that in the elastic deformation the correction factor can be computed from the following formula [9]: $(1 + S_p E_p / S_m E_m)$, where S_p is a cross sectional area of the plastic, S_m that of metal and E_p and E_m are elastic moduli of plastic and metal respectively. The correction factor used in this experiment is 1·02, which gives a negligible correction for the strain analysis under the elastic tensile deformation. For plastic deformation of metal, on the other hand, the correction must be larger than the above value, because a work hardening coefficient should be smaller than the elastic constant. At low temperature, in particular, the elastic constant of the photoelastic wafer increases with decreasing temperature, so that the reinforcement

effect becomes larger in the range of large plastic deformation. At –150°C for example, the shared load in photoelastic wafer reaches 5% of total load at the moment of cleavage fracture. However, the state of general yield below room temperature was always observed, when the plastic deformation attained only about 2% in principal strain difference. Therefore, reinforcement effect in such a small plastic strain is not so large. In this study, as the ratio of σ_N to σ_y is used as a basic parameter, then the reinforcement effect may be cancelled out.

Three types of propagating behaviour of the plastic zone in local yielding from a notch [10]: hinge type zone, 45° shear type zone and transition zone, have been observed. Similar observations of the plastic propagation from the notch root were also made in this experiment. At low stress level in the whole temperature range, it was observed that the plastic zone flowed about in 'hinge' type zone such as those deduced by the theoretical treatment under plane strain condition. At higher stress levels the plastic yielding at room temperature develops along the direction inclined at 45° to the tensile axis until the far-reaching plastic zone extends to the gross section of specimen. At low temperature, on the other hand, there appears no gross yielding, although the plastic propagation is the 45° shear type zone. Such 45° shear type zone is deduced from a theoretical treatment under plane stress condition. At low temperature, however, fracture occurs with increasing load, before the transition from the plastic hinge type zone to 45° shear type zone appears. Therefore, it may be considered that the plane strain assumption may be a most suitable approximation to the plastically constrained deformation.

Acknowledgements

The author wishes to express his appreciation to Professors Masahiko Suzuki and Takeo Yokobori, Tohoku University, for helpful discussions and suggestions. He also wishes to thank Messrs Masami Kikuchi and Tamotsu Tomobe for their experimental work.

References

1. OROWAN, E. 'Fracture and strength of solids', *Rep. Prog. Phys.*, vol. 12, p. 185, 1948.
2. DIXON, J. R. & VISSER, W. 'An investigation of elastic-plastic strain distribution around cracks in various sheet materials', Symposium on Photoelasticity (1961), Pergamon Press, London, pp. 231-250, 1963.
3. DIXON, J. R. 'Elastic-plastic strain distribution in flat bars containing holes or notches', *J. Mech. Phys. Solids*, vol. 10, p. 253, 1962.
4. KNOTT, J. F. & COTTRELL, A. H. 'Notch brittleness in mild steel', *J. Iron Steel Inst.*, vol. 201, p. 249, 1963.
5. ALLEN, N. P. 'Studies of the brittle fracture of steel during the past twenty years', Proceedings of International Conference on Fracture (1965), Sendai, Japanese Society for Strength and Fracture of Materials, p. 941, 1966.

6. WILSHAW, T. R. & PRATT, P. L. 'The effect of temperature and strain rate on the deformation and fracture of mild steel Charpy specimen', Proceedings of International Conference on Fracture (1965), Sendai, Japanese Society for Strength and Fracture of Materials, p. 973, 1966.
7. KNOTT, J. F. 'Some effects of hydrostatic tension on the fracture behaviour of mild steel', *J. Iron Steel Inst.*, vol. 204, p. 104, 1966.
8. TAKAHASHI, H. 'A liquid-air cryostat for photoelastic investigation', JSME 1967 Semi-International Symposium, Tokyo, Japanese Society of Mechanical Engineers, *Exp. Mech.*, vol. 2, p. 31, 1967.
9. ZANDMAN, F. 'Photoelastic-coating technique for determining stress distribution in welded structures', *Welding Res. Suppl.*, vol. 39, p. 191, 1960.
10. HAHN, G. T. & ROSENFIELD, A. R. 'Local yielding and extension of a crack under plane stress', *Acta Met.*, vol. 13, p. 293, 1965.

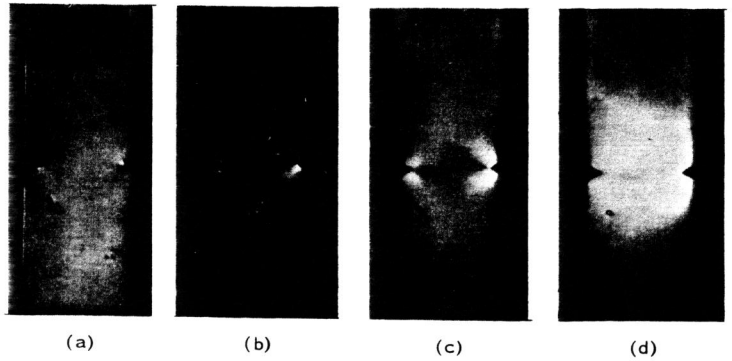

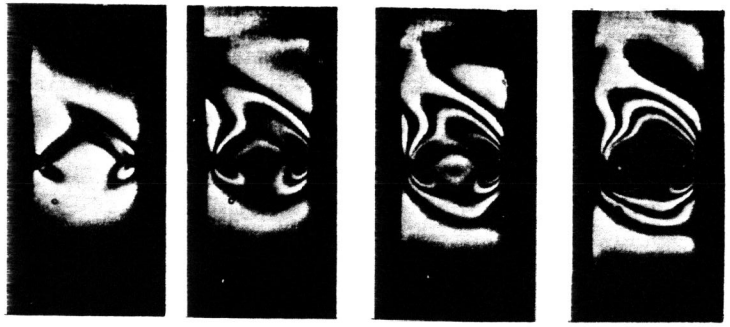

Fig. 1. Photoelastic fringe patterns (room temperature) (a) σ_N/σ_y = 0, (b) 1·0, (c) 1·15, (d) 1·25, (e) 1·30, (f) 1.35, (g) 1·37 and (h) 1·35.

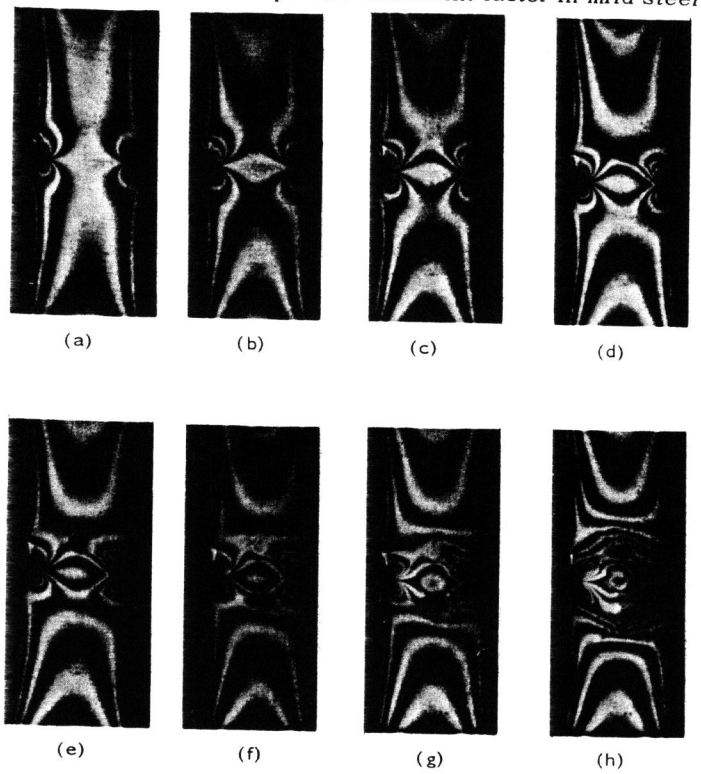

Fig. 2. Photoelastic fringe patterns (−150 C) (a) $\sigma_N/\sigma_y = 0$, (b) 1·0, (c) 1·16, (d) 1·19, (e) 1·20, (f) 1·20, (g) 1·20 and (h) 1·21.

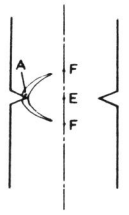

Fig. 3. Schematic diagram of plastic yielding.

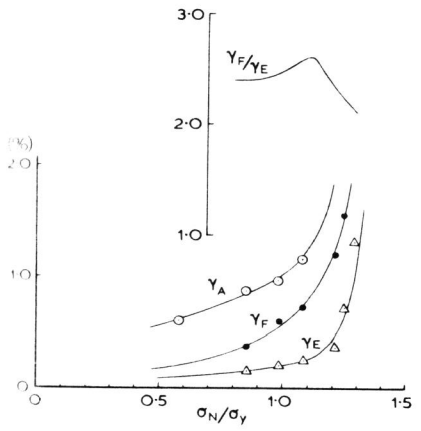

Fig. 4. Variation of principal strain difference at 'A', 'E' and 'F' (room temperature).

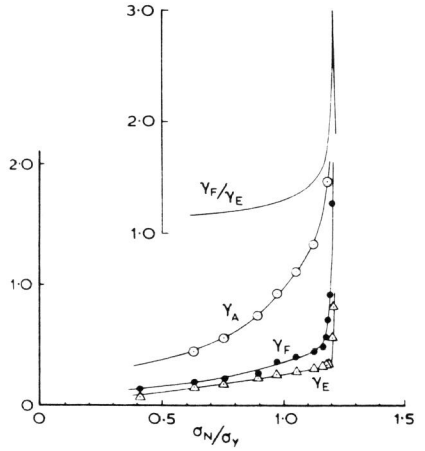

Fig. 5. Variation of principal strain difference at 'A', 'E' and 'F' (−150°C).

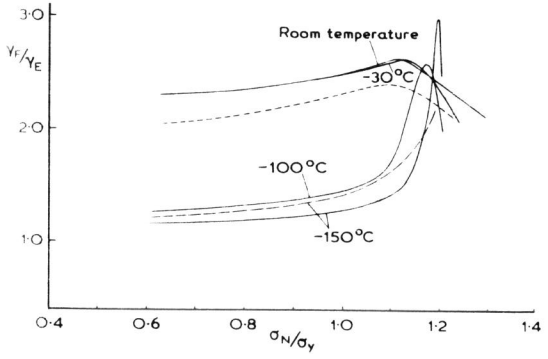

Fig. 6. Temperature dependence of strain ratio curve; γ_F $\gamma_E - \sigma_N$ σ_y (steel A).

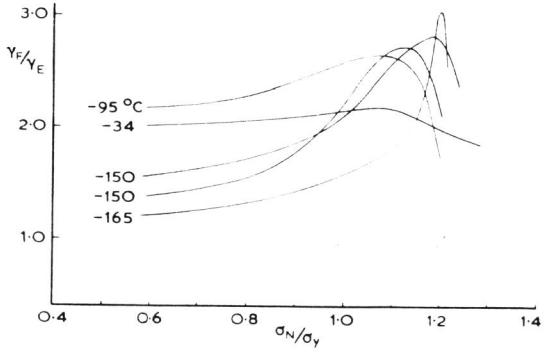

Fig. 7. Temperature dependence of strain ratio curve; γ_F/γ_E σ_N/σ_y (steel B).

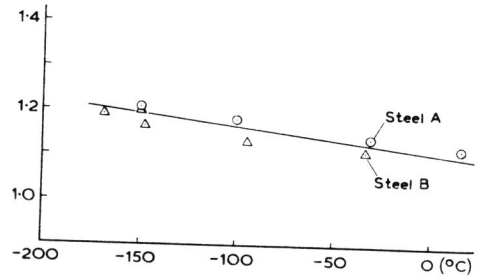

Fig. 8. Temperature dependence of plastic constraint factor; ⊙ steel A and △ steel B.

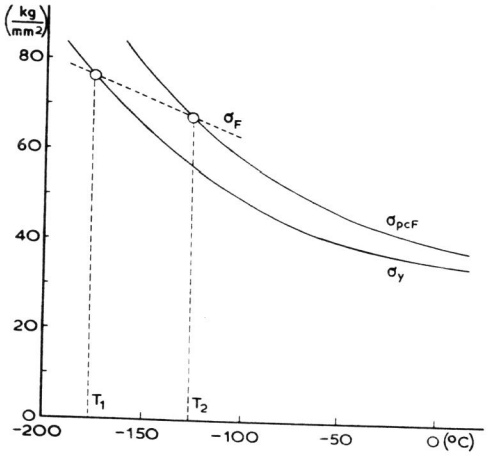

Fig. 9. Explanation of transition temperature: σ_y is the uniaxial and σ_{pcF} the notch-constrained yield stress and σ_F the fracture stress for cleavage fracture.

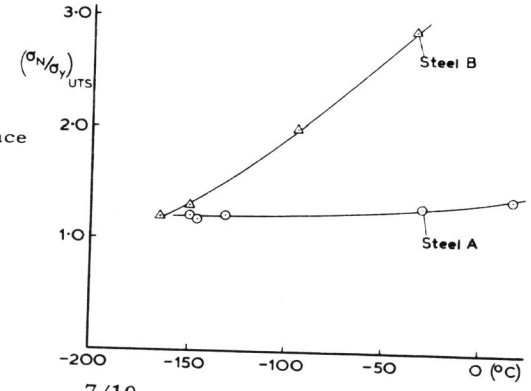

Fig. 10. Temperature dependence of nominal ultimate tensile strength $(\sigma_N/\sigma_y)_{UTS}$; ⊙ steel A and △ steel B.